Interference Management Through Exclusion Zones in Two-Tier Cognitive Networks

Utku Tefek, *Student Member, IEEE*, and Teng Joon Lim, *Senior Member, IEEE*

***Abstract*—The transmission capacity of wireless networks is limited by the intensity of the interference received from concurrent transmissions. Interference causes serious performance degradation, particularly when no centralized controller within the network exists. Cognitive radio (CR) is a promising solution for distributed interference management as users with CR capabilities can acquire local activity and position information to achieve spatial reuse while limiting interference to neighboring users. Considering a two-tier network consisting of a licensed primary network overlaid by an unlicensed secondary tier, this paper proposes CR-based spectrum access schemes for secondary users (SUs). Acquiring the activity information of nearby users, the SUs are activated only when they are outside the exclusion zone of primary receivers. Additionally, the active secondary transmitters are separated from each other by forming secondary exclusion zones around themselves. Using stochastic geometry, primary and secondary exclusion zone sizes that maximize the transmission capacity under per-tier outage constraints are calculated. Analytical results supported by numerical simulations, suggest primary exclusion zones reduce predominantly the cross-tier interference while the secondary exclusion zone size is critical in mitigating the interference among SUs.**

***Index Terms*—Cognitive radio, exclusion zone, guard zone, interference management, Poisson point process, spectrum sharing, stochastic geometry.**

I. Introduction

In a wireless environment with a dense deployment of mobile and fixed nodes, it is critical to control the interference levels seen by all nodes to achieve acceptable network performance. Various forms of smart resource allocation, including the partitioning of time and/or frequency resources and cell size adaptation, have been proposed for interference management. In this paper, we consider a deployment with two co-existing systems, where one has a lower priority to use the channel resources. This corresponds for instance to machine-to-machine (M2M) networks operating together with a conventional cellular network. In such a scenario, we propose to use cognitive radio (CR) techniques in the secondary tier for interference management.

In the underlay type of CR [1], secondary users (SUs) communicate with each other without causing excessive interference to licensed primary users (PUs) or other SUs. Since the interference is highly dependent on the distance, the CR mechanism can be used to implement a simple location-based strategy: transmit when nearby PUs are sensed to be inactive. This configuration can also be interpreted as virtual exclusion zones around PUs where interfering SUs are deactivated. However, concurrent transmissions of several distant SUs on the same spectrum band may still cause unacceptable interference and thus aggregate interference from all transmitters needs to be calculated. In modeling the aggregate interference, the spatial distribution of the active nodes plays a critical role. Due to the location uncertainty or mobility of the nodes in a typical network, stochastic geometry analysis is a powerful tool in calculating the aggregate interference, as it accounts for the entire space of all possible node locations in a probabilistic manner.

Stochastic geometry has been widely used to analyze the performance of ad-hoc, cellular and cognitive networks thanks to its tractable models to characterize interference in large-scale dense wireless networks. The related work can be outlined as follows. The transmission capacity of single-tier ad-hoc networks under outage constraints were first analyzed in [2] assuming a simple ALOHA-type MAC protocol. Here, the transmission capacity (also known as spectral efficiency) is defined as the maximum allowable density of simultaneous transmissions to maintain a certain signal to interference-plus-noise ratio (SINR). Then, the concept of exclusion zone was introduced for ad-hoc networks in [3] to achieve higher capacity by spatially sharing the spectrum. The implementation of the exclusion zone requires *cognition* for the transmitter node to acquire activity and position information of nearby transmitters or receivers [4], [5]. Following [3], the exclusion zone has been successfully employed in ad-hoc [6]–[9] and heterogeneous cellular networks [10]–[13] to enhance the spatial reuse of the spectrum bands.

In two-tier networks, it is also necessary to mitigate cross-tier interference. SUs typically perform spectrum sensing [14] to obtain the activity information of nearby PUs and inhibit their own transmissions upon detection of a primary beacon. Hong *et al.* [15], Vu *et al.* [16] and Ghasemi and Sousa [17] focused on the aggregate interference in the context of a spectrum sensing CRN, where the transmissions of the SUs within the circular primary exclusion zone are suppressed. However, [15] and [17] assume only a single primary transmitter-receiver pair while [16] assumes a single primary transmitter broadcasting to surrounding primary receivers. A more realistic sensing mechanism with non-circular exclusion zones is used in [18], but the authors did not consider the secondary network outage probability. Lee and Haenggi [19] derived bounds on the primary

Manuscript received February 11, 2015; revised September 4, 2015; accepted November 15, 2015. Date of publication November 20, 2015; date of current version March 8, 2016. The associate editor coordinating the review of this paper and approving it for publication was T. Taleb.

The authors are with the Department of Electrical and Computer Engineering, National University of Singapore, Singapore 138601 (e-mail: utku@u.nus.edu; eleltj@nus.edu.sg).

Color versions of one or more of the figures in this paper are available online at http://ieeexplore.ieee.org.

Digital Object Identifier 10.1109/TWC.2015.2502254

and secondary outage probabilities by analyzing the aggregate interference in an underlay type CRN with multiple PU and SU pairs. Primary receivers were protected from the secondary transmitters by the primary exclusion zones, but spectrum sharing within the secondary network is not considered. In fact, as will be shown in this paper, introducing the primary exclusion zone alone does not improve the spectral efficiency considerably, particularly when the interference received at a secondary receiver is dominated by the interference from other SUs.

This paper analyzes and designs spatial spectrum sharing schemes for two-tier cognitive networks, in which the spectrum is shared between SUs and PUs, as well as among SUs. The maximum density of active secondary transmitters satisfying the primary and secondary outage constraints is analyzed for three different scenarios.

1) *Baseline scheme*—-A simple underlay scheme is presented for comparison purposes where the secondary transmitters are distributed according to a homogeneous Poisson Point Process (PPP) as defined in A.1.2 in [20]. Each secondary transmitter is retained active independently with a certain transmit probability to avoid creating excessive interference to other users.
2) *Scheme I*—This model assumes exclusion zones around primary receivers. Secondary transmitters in the vicinity of the primary receivers deactivate themselves, and it becomes less likely for an SU to cause harmful interference to a primary receiver. The exclusion zone model introduced here is different from that of any previous work, in the sense that each secondary transmitter outside the exclusion zones transmits with a probability $p_t \leq 1$. We derive the primary and secondary outage probabilities in terms of primary exclusion zone radius r_e and transmission probability p_t. Then r_e and p_t are jointly designed to achieve the highest density of active secondary transmitters under per-tier outage constraints.
3) *Scheme II*—In this most advanced model, in addition to the primary exclusion zones, concurrent transmissions from nearby secondary transmitters are prohibited thanks to the exclusion zones around the active secondary transmitters. As shown in Figure 1, the secondary exclusion zone inhibits secondary transmitters in the vicinity of an active secondary transmitter. Large exclusion zones, therefore decrease the interference at the cost of a reduced spatial reuse. We investigate the optimal primary and secondary exclusion zone radii (i.e., r_e and r_g) to maximize the active secondary transmitter density without violating per-tier outage constraints.

Table I outlines the studied sharing schemes which together provide insights for researchers and MAC protocol designers to jointly design transmit probability and primary/secondary exclusion zone radii in two-tier cognitive networks.

II. System Model

We consider a densely deployed secondary network that shares the same frequency band with the primary network. The primary and secondary transmitters are assumed to form two independent homogeneous spatial PPPs, where $\Phi_p = \{x_i\}$ and $\Phi_s = \{y_i\}$ with intensities λ_p, λ_s respectively. The primary and secondary receivers are located at maximum distances of r_p and r_s from their respective transmitters. All primary and active secondary transmitters employ transmission powers P_p and P_s respectively. The activation of the SUs depends on the channel access/sharing scheme of the secondary transmitters. Although we consider sharing schemes over a single time-frequency block of spectrum resources, the presented schemes can be applied to each resource block independently. Thus, a secondary transmitter within the exclusion zone of a primary receiver in a particular resource block can still have a transmission opportunity in orthogonal resource blocks.

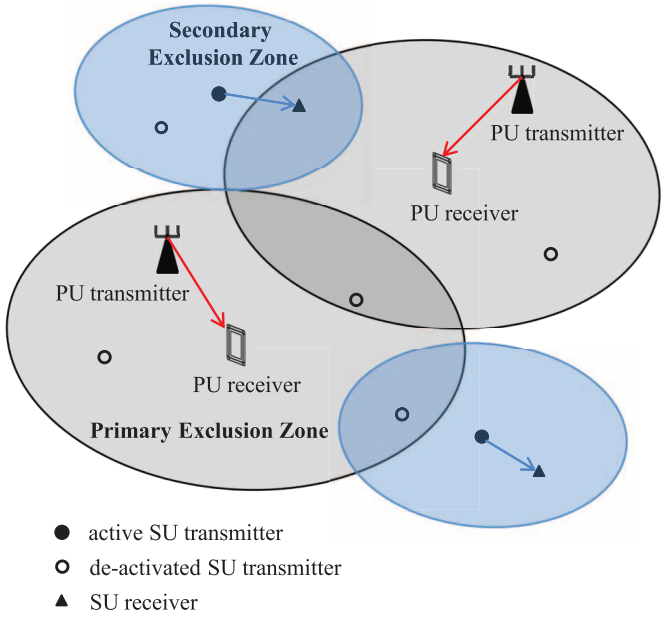

Fig. 1. Two-tier network model in scheme II.

TABLE I
Spectrum Sharing Schemes

Schemes	Transmission prob. outside the excl. zones	Primary excl. zone exists	Secondary excl. zone exists
Baseline	$p_t \leq 1$	–	–
Scheme I	$p_t \leq 1$	Yes	–
Scheme II	1	Yes	Yes

The path-loss attenuation at a point y from a transmitter at x is modeled by $l(x, y) = \|y - x\|^{-\alpha}$ where α is the path loss exponent. Hence, aggregate interference from the process Φ at the point y is represented by $I(y) = \sum_{x \in \Phi} P_x h_x l(x, y)$, where the transmit power P_x is either P_p or P_s depending on the type of transmitter, and h_x is the unit mean exponential random variable (Rayleigh fading) representing the small-scale fading gain. We assume h_x to be i.i.d. across all users. For each discussed scheme, four types of aggregate interference are considered: PUs to PUs $I_{p,p}$, PUs to SUs $I_{p,s}$, SUs to SUs $I_{s,s}$ and SUs to PUs $I_{s,p}$.

For a given target outage probability ϵ, the transmission capacity of a wireless network can be quantified by the spatial intensity of the attempted transmissions λ_ϵ, multiplied by the associated success probability [21], i.e. $C = (1 - \epsilon)\lambda_\epsilon$. Therefore, to maximize the secondary network capacity, we

calculate the maximum allowable density of active secondary transmitters that satisfies the outage constraints. Note that, the outage constraints for both primary and secondary networks must be satisfied.

III. Baseline Scheme—Simple Underlay

In simple underlay, we adopt an ALOHA type protocol, where each SU transmits with a certain probability p_t regardless of the activity of nearby PUs. Since each SU independently decides on its transmission, the distribution of active SUs is still a homogeneous PPP with intensity $\lambda_s p_t$. To guarantee quality of service (QoS) for all primary and secondary receivers located at maximum distance from their transmitters, the corresponding SINR ratios should be probabilistically greater than a threshold.

Without loss of generality, a primary receiver is assumed to be at the origin. Its transmitter located at x_0, is assumed to be located at a distance of r_p away, making this the worst-case scenario in terms of received signal strength for the primary receiver. The outage probability constraint can be expressed as

$$\Pr\left(\frac{h_p P_p r_p^{-\alpha}}{N_0 + I_{s,p} + I_{p,p}} \geq \eta_p\right) \geq 1 - \epsilon_p \tag{1}$$

where $I_{s,p} = \sum_{y_i \in \Phi_s^{p_t}} P_s h_{y_i} \|y_i\|^{-\alpha}$ is the aggregate interference from active secondary transmitters, each of which transmits with probability p_t and $I_{p,p} = \sum_{x_i \in \Phi_p \setminus \{x_0\}} P_p h_{x_i} \|x_i\|^{-\alpha}$ is the aggregate interference from primary transmitters. N_0 is the background noise power, η_p is the SINR threshold for successful transmission, and ϵ_p is the maximum allowable outage probability for the PUs. Note that, $\Phi_s^{p_t}$ is a homogeneous PPP since it is obtained from the independent thinning of Φ_s. $\Phi_p \setminus \{x_0\}$ is also a homogeneous PPP by Slivnyak's theorem [22]. Assuming that λ_s is sufficiently large, we state Lemma 1 and Lemma 2.

Lemma 1: The maximum density of active secondary transmitters satisfying the primary outage constraint is

$$\tilde{\lambda}_s = -\frac{P_p^\delta}{P_s^\delta \eta_p^\delta r_p^2 K_\alpha}\left[\ln(1-\epsilon_p) + \frac{\eta_p N_0}{P_p r_p^{-\alpha}}\right] - \lambda_p \frac{P_p^\delta}{P_s^\delta} \tag{2}$$

and the optimal transmission probability is $\tilde{p}_t = \tilde{\lambda}_s / \lambda_s$, where $K_\alpha = 2\pi^2/[\alpha \sin(2\pi/\alpha)]$ and $\delta = 2/\alpha$.

The proof is provided in Appendix A.

A similar outage constraint applies for a typical secondary receiver assumed to be located at the origin,

$$\Pr\left(\frac{h_s P_s r_s^{-\alpha}}{N_0 + I_{s,s} + I_{p,s}} \geq \eta_s\right) \geq 1 - \epsilon_s \tag{3}$$

where η_s is the SINR threshold, and ϵ_s is the outage probability for the SUs. The aggregate interference from the active secondary transmitters transmitting with probability $\bar{p}_t$ is $I_{s,s} = \sum_{y_i \in \Phi_s^{p_t} \setminus \{y_0\}} P_s h_{y_i} \|y_i\|^{-\alpha}$ and the aggregate interference from the primary transmitters $I_{p,s}$ is statistically identical to $I_{p,p}$, i.e., $I_{p,s} = \sum_{x_i \in \Phi_p} P_p h_{x_i} \|x_i\|^{-\alpha}$.

Lemma 2: The maximum density of active secondary transmitters satisfying the secondary outage constraint is

$$\bar{\lambda}_s = -\frac{\ln(1-\epsilon_s) + \frac{\eta_s N_0}{P_s r_s^{-\alpha}}}{\eta_s^\delta r_s^2 K_\alpha} - \lambda_p \frac{P_p^\delta}{P_s^\delta} \tag{4}$$

and the optimal transmission probability is $\bar{p}_t = \bar{\lambda}_s / \lambda_s$.

The proof is given in Appendix B.

Based on Lemma 1 and Lemma 2, the maximum active secondary transmitter density should be $\min\{\tilde{\lambda}_s, \bar{\lambda}_s\}$ and the transmission probability $p_t = \min\{\tilde{\lambda}_s, \bar{\lambda}_s\}/\lambda_s$ to ensure the interference from the secondary transmitters does not violate the primary and secondary outage constraints. Since we did not consider any spatial spectrum sharing scheme, transmission capacity of the secondary network in a simple underlay scheme is typically low. On the other hand, the implementation is easy as the secondary nodes require only the overall density of primary and secondary transmitters to calculate the transmission probability p_t.

IV. Scheme I—Primary Exclusion Zone

In this section, we consider circular exclusion zones with radius r_e around each primary receiver, where SUs are not allowed to transmit. By deactivating the secondary transmitters in the vicinity of primary receivers, dominant interferers can be suppressed and hence a greater density of SUs (outside the exclusion zones) can be kept active without violating the primary outage constraint. Besides, the secondary receivers can be kept apart from the primary transmitters by a certain distance and protected from the PU transmissions. Reliably detecting any active PUs requires cognition in the secondary transmitters. In this scheme, we adopt the beacon sensing technique presented in [4], [17]. In beacon sensing, primary receivers broadcast an inhibitory beacon signal on an out-of-band control channel. The cognitive transmitters listen to the control channel and cease their transmissions upon detection of a primary beacon signal. This technique ensures approximately circular exclusion zones around primary receivers. If no beacon is detected, the secondary transmitter transmits with probability p_t. Note that the exclusion zone introduced here is different from that of [15]–[17], [19] and [23], in which SU transmitters outside the primary exclusion zones transmit with probability 1. In fact, that is a special case of the proposed model with $p_t = 1$. The design problem in this proposed scheme is therefore, to jointly optimize p_t and r_e for maximum secondary network capacity under outage constraints.

The probability of staying active for a secondary transmitter y_i is equal to the probability that there is no primary receiver within distance r_e, i.e. p_e, multiplied by p_t. Thus, we calculate the retaining probability for an SU transmitter as,

$$p_r = p_e p_t = \exp(-\lambda_p \pi r_e^2) p_t. \tag{5}$$

We first consider the primary outage constraint. The distribution of $I_{p,p}$ is the same as in the simple underlay case because the channel access scheme of PUs is the same. Aggregate interference from the active secondary transmitters to a primary

receiver can be expressed as, $I_{s,p} = \sum_{y_i \in \Phi_s^{p_t,r_e}} P_s h_{y_i} \|y_i\|^{-\alpha}$ where $\Phi_s^{p_t,r_e}$ represents the locations of the SU transmitters outside the primary exclusion zones of radius r_e, each selected with probability p_t. The PDF of $I_{s,p}$ or its Laplace transform $\mathcal{L}_{I_{s,p}}(s)$ cannot be calculated exactly since $\Phi_s^{p_t,r_e}$ is a PHP obtained from the independent thinning of Φ_s to $\Phi_s^{p_t}$, and then location dependent thinning of $\Phi_s^{p_t}$ to $\Phi_s^{p_t,r_e}$. Instead we propose a lower bound for the active SU transmitter density by making the following approximation. We assume that the active secondary transmitters have zero density in a disk centered at the typical primary receiver, and are homogeneously distributed with density $\lambda_s p_t$ elsewhere. In other words, we treat the secondary transmitters within the exclusion zones of other primary receivers (other than the typical primary receiver) as if they are active with probability p_t. Let us denote the locations of the active secondary transmitters resulting from this approximation by Φ_s^a. Since $\Phi_s^{p_t,r_e} \subseteq \Phi_s^a$, the interference caused by Φ_s^a stochastically dominates[1] the interference caused by $\Phi_s^{p_t,r_e}$. Therefore, the larger interference caused by Φ_s^a in the assumption leads to an upper bound on the outage probability, and hence a lower bound on the density of active secondary transmitters.

Similar approximations were made in [19], [23] and verified by simulations in [19]. By replacing $\Phi_s^{p_t,r_e}$ with Φ_s^a in $I_{s,p}$, the left-hand side of the primary outage constraint (1) can be expressed as,

$$\begin{aligned}
&\exp\left(-\frac{\eta_p N_0}{P_p r_p^{-\alpha}}\right)\mathcal{L}_{I_{s,p}}\left(\frac{\eta_p}{P_p r_p^{-\alpha}}\right)\mathcal{L}_{I_{p,p}}\left(\frac{\eta_p}{P_p r_p^{-\alpha}}\right)\\
&= \exp\left(\frac{-\eta_p N_0}{P_p r_p^{-\alpha}}\right)\exp\left(-2\pi\lambda_s p_t \int_{r_e}^{\infty} \frac{r}{1+\frac{r^\alpha P_p r_p^{-\alpha}}{\eta_p P_s}} dr\right)\\
&\quad \times \exp(-\lambda_p \eta_p^\delta r_p^2 K_\alpha). \qquad (6)
\end{aligned}$$

Simplifying (6) with $\alpha = 4$, the relation between the exclusion zone radius r_e and the transmission probability p_t satisfying the primary outage constraint is,

$$\begin{aligned}
1-\epsilon_p \le{}& \exp\left(\frac{-\eta_p N_0}{P_p r_p^{-4}}\right)\exp\left(-\frac{\pi^2}{2}\lambda_p\sqrt{\eta_p} r_p^2\right)\\
&\times \exp\left\{-r_p^2\left(\frac{\eta_p P_s}{P_p}\right)^{\frac{1}{2}}\lambda_s p_t\right.\\
&\left.\times\left[\frac{\pi^2}{2} - \pi\tan^{-1}\left(\frac{r_e^2}{r_p^2}\left(\frac{P_p}{\eta_p P_s}\right)^{\frac{1}{2}}\right)\right]\right\}. \qquad (7)
\end{aligned}$$

Now, we consider the interference to the SUs and the secondary outage constraint. The interference from the active SU transmitters cannot be calculated exactly due to the location dependent thinning of Φ_s to $\Phi_s^{p_t,r_e}$. Nevertheless, similar to approximating $\Phi_s^{p_t,r_e}$ to Φ_s^a above, we model the active SU transmitters seen by an active SU receiver by a homogeneous PPP of density $\lambda_s p_t$. As $\Phi_s^{p_t,r_e} \subseteq \Phi_s^{p_t}$, the interference caused by $\Phi_s^{p_t}$ stochastically dominates the interference from the active SUs located at $\Phi_s^{p_t,r_e}$.

Finally, we upper bound the interference from the PUs to the SUs. Due to the exclusion zones of radius r_e around primary receivers and the distance r_p between the primary transmitter-receiver pairs, an active SU transmitter cannot be closer than $r_e - r_p$ to a primary transmitter. Given the distance of r_s between the secondary transmitter-receiver pairs, the distance between an active secondary receiver and a primary transmitter is at least $r_e - r_p - r_s$. [2] Let us denote the homogeneous PPP of density λ_p outside a disk of radius $r_e - r_p - r_s$ centered at a secondary receiver as $\Phi_p^{r_e-r_p-r_s}$. Since the density of primary transmitters ranging from distance $r_e - r_p - r_s$ to $r_e + r_p + r_s$ away from an active secondary receiver is actually less than λ_p, $I_{p,s}$ is stochastically dominated by the interference caused by $\Phi_p^{r_e-r_p-r_s}$. Based on these upper bounds on the interference to the SUs, we can express the left-hand side of the secondary outage constraint (3) as,

$$\begin{aligned}
&\exp\left(-\frac{\eta_s N_0}{P_s r_s^{-\alpha}}\right)\mathcal{L}_{I_{s,s}}\left(\frac{\eta_s}{P_s r_s^{-\alpha}}\right)\mathcal{L}_{I_{p,s}}\left(\frac{\eta_s}{P_s r_s^{-\alpha}}\right)\\
&= \exp\left(\frac{-\eta_s N_0}{P_s r_s^{-\alpha}}\right)\exp\left(-\lambda_s p_t \eta_s^\delta r_s^2 K_\alpha\right)\\
&\quad \times \exp\left(-2\pi\lambda_p \int_{r_e-r_p-r_s}^{\infty} \frac{r}{1+\frac{r^\alpha P_s r_s^{-\alpha}}{\eta_s P_p}} dr\right). \qquad (8)
\end{aligned}$$

With $\alpha = 4$, the radius of the primary exclusion zone satisfying the secondary outage constraint is bounded as follows,

$$\begin{aligned}
1-\epsilon_s \le{}& \exp\left(-\frac{\eta_s N_0}{P_s r_s^{-4}}\right)\exp\left(-\frac{\pi^2}{2}\lambda_s p_t\sqrt{\eta_s} r_s^2\right)\\
&\times \exp\left\{-r_s^2\left(\frac{\eta_s P_p}{P_s}\right)^{\frac{1}{2}}\lambda_p\right.\\
&\left.\times\left[\frac{\pi^2}{2} - \pi\tan^{-1}\left(\left(\frac{r_e-r_p-r_s}{r_s}\right)^2\left(\frac{P_s}{\eta_s P_p}\right)^{\frac{1}{2}}\right)\right]\right\}. \qquad (9)
\end{aligned}$$

Inequalities (7) and (9) give the bounds on the design variables p_t and r_e to avoid violating the primary and secondary outage constraints respectively. Let us express inequality (7) resulting from the primary outage constraint in the form of $P_1(p_t, r_e) \ge 0$, and inequality (9) resulting from the secondary outage constraint as $S_1(p_t, r_e) \ge 0$. Then, the objective is to select a feasible (p_t, r_e) pair that maximizes the density of active secondary transmitters $\lambda_s p_r$, or equivalently the retaining probability $p_r = \exp(-\lambda_p \pi r_e^2) p_t$ as calculated above. The following problem describes this objective.

Problem 1:

$$\max_{1\ge p_t\ge 0,\ r_e^{max}\ge r_e\ge r_p+r_s} p_r(p_t, r_e) = \exp(-\lambda_p\pi r_e^2)p_t$$

[1] A random variable X stochastically dominates another random variable Y if $\Pr(X > c) \ge \Pr(Y > c), \forall c$.

[2] We assume that r_e is larger than $r_p + r_s$ to ensure a certain separation between the primary transmitters and secondary receivers.

subject to,

$$P_1(p_t, r_e) \geq 0$$
$$S_1(p_t, r_e) \geq 0.$$

Here, r_e^{max} is the physical upper bound on the exclusion zone radius beyond which the primary beacon cannot be detected by the secondary transmitters. We propose a solution to Problem 1, by making the following observations. First, we assume that $P_1(0, r_e) \geq 0$ and $S_1(0, r_e) \geq 0$ are satisfied $\forall r_e \in [r_p + r_s, r_e^{max}]$. This assumption ensures that Problem 1 is feasible (i.e. it has a solution). Then, note that $P_1(p_t, r_e)$ and $S_1(p_t, r_e)$ are monotone decreasing functions of p_t. Therefore, there exists a smallest upper bound $M(r_e) \geq 0$ for p_t such that $p_t \in [0, M(r_e)]$ satisfies $P_1(p_t, r_e) \geq 0$ and $S_1(p_t, r_e) \geq 0$, while $p_t > M(r_e)$ violates at least one of these constraints or the implicit constraint $p_t \in [0, 1]$. From (7) and (9) we calculate the smallest upper bound $M(r_e)$ in equation (10). That is,

$$M(r_e) = \min \left\{ -\frac{\frac{\eta_p N_0}{P_p r_p^{-4}} + \frac{\pi^2}{2}\lambda_p \sqrt{\eta_p} r_p^2 + \ln(1-\epsilon_p)}{r_p^2 \left(\frac{\eta_p P_s}{P_p}\right)^{\frac{1}{2}} \lambda_s \left[\frac{\pi^2}{2} - \pi \tan^{-1}\left(\frac{r_e^2}{r_p^2}\left(\frac{P_p}{\eta_p P_s}\right)^{\frac{1}{2}}\right)\right]}, \right.$$
$$\left. \left(\frac{P_p}{P_s}\right)^{\frac{1}{2}} \frac{\lambda_p}{\lambda_s}\left[\frac{2}{\pi}\tan^{-1}\left(\left(\frac{r_e - r_p - r_s}{r_s}\right)^2 \left(\frac{P_s}{\eta_s P_p}\right)^{\frac{1}{2}}\right) - 1\right] \right.$$
$$\left. -\frac{\frac{\eta_s N_0}{P_s r_s^{-4}} + \ln(1-\epsilon_s)}{\frac{\pi^2}{2}\lambda_s \sqrt{\eta_s} r_s^2}, 1 \right\}. \quad (10)$$

Based on $M(r_e)$ we state the following lemma.

Lemma 3: The optimal point, maximizing the retaining probability p_r, lies on the boundary of the feasible region described by the points $(M(r_e), r_e), \forall r_e \in [r_p + r_s, r_e^{max}]$.

Proof: Let us assume the contrary where the optimal point (p_t', r_e') is strictly inside the feasible region such that $p_t' < M(r_e')$. Then, there exist some larger $p_t'' \in (p_t', M(r_e')]$ such that (p_t'', r_e') is feasible. Since the objective $p_r(p_t, r_e)$ is a monotone increasing function of p_t, $p_r(p_t'', r_e') > p_r(p_t', r_e')$ and (p_t', r_e') is not optimal. ■

Based on Lemma 3, problem 1 can be easily solved numerically by calculating $p_r(p_t, r_e)$ values over the points $(M(r_e), r_e)$, $\forall r_e \in [r_p + r_s, r_{max}]$. This is illustrated in Figure 2, where the contour plot represents the isometric transmission capacity $(1-\epsilon_s)\lambda_s p_r$ curves decreasing from red to blue and the black curve is $M(r_e)$. Unlike the previous work practicing $p_t = 1$, the fact that the optimal value of p_t with given parameters is around 0.026 reflects the necessity of optimizing p_t and r_e jointly.

Note that, since we used the stochastically dominating values of the interferences $I_{s,p}$, $I_{s,s}$ and $I_{p,s}$ in deriving the inequalities (7) and (9), the maximum value of p_r in the solution of Problem 1 is in fact a lower bound on the retaining probability. This lower bound is tighter for smaller r_e because the PHP $\Phi_s^{p_t, r_e}$ converges to a homogeneous PPP as r_e decreases.

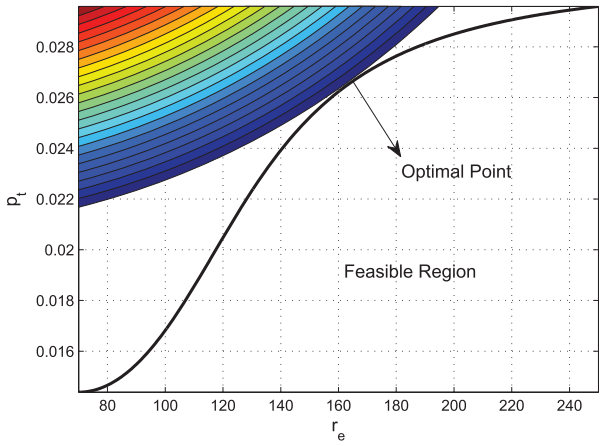

Fig. 2. The contour plot of the transmission capacity (decreases from red to blue) and the boundary of the feasible region $p_t = M(r_e)$. The parameters are $P_p = 3$ W, $P_s = 0.1$ W, $\lambda_p = 3 \times 10^{-6}$, $\lambda_s = 10^{-3}$, $N = 10^{-12}$ W, $\alpha = 4$, $r_p = 50$ m, $r_s = 20$ m, $\epsilon_p = 0.1$, $\epsilon_s = 0.1$ $\eta_p = \eta_s = 3$.

V. Scheme II—Primary and Secondary Exclusion Zone

Although the primary exclusion zone can reduce the interference across the primary and secondary networks, it does not provide any spatial spectrum sharing protocol within the secondary tier. Furthermore, given the same active SU density, active secondary transmitters in the presence of primary exclusion zones are concentrated in a smaller region, i.e., outside the exclusion zones, and cause more interference to each other as compared to the case of simple underlay. This arises from the fact that the mean interference between the nodes distributed according to a PHP is larger than that of nodes following a homogeneous PPP of the same density [20]. Consequently, the active secondary transmitter density is limited by the interference $I_{s,s}$ received from concurrent secondary transmissions.

To mitigate the interference between SUs, we combine the primary exclusion zones with secondary exclusion zones. Instead of using a generalized transmit probability to independently deactivate SUs with probability p_t (Scheme I), the transmission probability of a secondary transmitter in this scheme is inversely related to the number of other secondary transmitters within its exclusion zone. The implementation of the secondary exclusion zone requires CR techniques to acquire local activity and position information of neighboring secondary transmitters. In particular, each secondary transmitter generates a uniformly distributed random number between 0 and 1, and exchanges this mark with neighboring SUs within its exclusion zone of radius r_g. Thus, each secondary transmitter receives a set of random marks from its neighbors within a distance of r_g. A secondary transmitter participates in the data transmission process if its own generated mark is smaller than each of the received marks.

The retaining probability for a node y_i after the secondary exclusion zone of radius r_g is introduced can be expressed as,

$$p_g = \int_0^1 \exp(-\lambda_s \pi r_g^2 u) du = \frac{1 - \exp(-\lambda_s \pi r_g^2)}{\lambda_s \pi r_g^2} \quad (11)$$

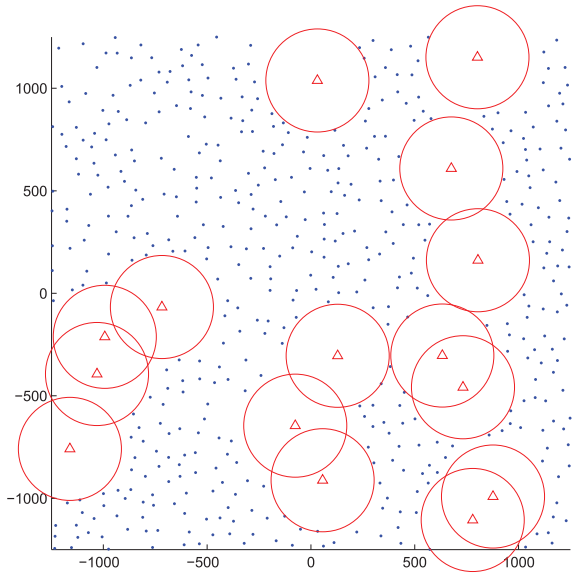

Fig. 3. Secondary transmitters forming a MHP with holes. Blue dots are active secondary transmitters, red triangles are primary receivers and large red circles represent the virtual boundaries of primary exclusion zones.

where $\exp(-\lambda_s \pi r_g^2 u)$ is the probability that no other node with a smaller mark exists within a distance of r_g to y_i, conditioned on the mark of y_i is u. The introduction of the secondary exclusion zones results in an active secondary transmitter distribution based on a type II Matérn Hard Core Process (MHP) [24].

The node y_i is outside the primary exclusion zones with probability $p_e = \exp(-\lambda_p \pi r_e^2)$. Since the locations of the PUs and SUs follow two independent processes, secondary and primary exclusion zones are formed independently. Thus, the ultimate retaining probability p_r for node y_i can be obtained from the multiplication of the independent retaining probabilities p_g from (11) and p_e as follows,

$$p_r = p_g p_e = \frac{1-\exp(-\lambda_s \pi r_g^2)}{\lambda_s \pi r_g^2} \exp(-\lambda_p \pi r_e^2). \tag{12}$$

The spatial distribution of the active secondary transmissions in this scheme can be thought of a type II MHP with holes centered at primary receivers. An example realization is shown in Figure 3. Notice that the SUs are distributed rather uniformly outside the primary exclusion zones to reduce interference within the secondary network.

After expressing p_r in terms of r_g and r_e, we proceed to calculate the outage probability expressions. Regarding the primary outage constraint, $I_{p,p}$ is the same as calculated in the previous sections. However, the point process of active secondary transmitters $\Phi_s^{r_g,r_e}$ does not follow any known spatial distribution. Given the original process of secondary transmitters Φ_s, let us define $\Phi_s^{r_g}$ as the MHP generated from Φ_s based on a *hard-core* distance of r_g after the secondary exclusion zones are introduced. Then, $\Phi_s^{r_g,r_e} \subseteq \Phi_s^{r_g} \subseteq \Phi_s$. As proved in [25], a type II MHP can be safely approximated as a PPP since the ratio of the mean interference in a MHP of density λ_s and *hard-core* distance r_g, to a PPP of density $\lambda_s p_g$ never exceeds 1 dB. Thus, we can closely approximate $\Phi_s^{r_g}$ by a PPP of density $\lambda_s p_g$. For a typical primary receiver, there cannot be any secondary interferers within distance r_e. Therefore, we model the secondary transmitters seen by a primary receiver as a homogeneous PPP of density $\lambda_s p_g$ outside its exclusion zone, and zero density inside the exclusion zone. Hence, the left-hand side of the primary outage constraint (1) can be approximated to,

$$\begin{aligned}
&\exp\left(-\frac{\eta_p N_0}{P_p r_p^{-\alpha}}\right) \mathcal{L}_{I_{s,p}}\left(\frac{\eta_p}{P_p r_p^{-\alpha}}\right) \mathcal{L}_{I_{p,p}}\left(\frac{\eta_p}{P_p r_p^{-\alpha}}\right) \\
&= \exp\left(\frac{-\eta_p N_0}{P_p r_p^{-\alpha}}\right) \exp\left(-2\pi\lambda_s p_g \int_{r_e}^{\infty} \frac{r}{1+\frac{r^\alpha P_p r_p^{-\alpha}}{\eta_p P_s}} dr\right) \\
&\quad \times \exp(-\lambda_p \eta_p^\delta r_p^2 K_\alpha).
\end{aligned} \tag{13}$$

Setting $\alpha = 4$ yields,

$$\begin{aligned}
1-\epsilon_p \le \exp\left(\frac{-\eta_p N_0}{P_p r_p^{-4}}\right) &\exp\left(-\frac{\pi^2}{2}\lambda_p \sqrt{\eta_p} r_p^2\right) \\
&\times \exp\left\{-r_p^2\left(\frac{\eta_p P_s}{P_p}\right)^{\frac{1}{2}} \lambda_s \frac{1-\exp(-\lambda_s \pi r_g^2)}{\lambda_s \pi r_g^2}\right. \\
&\left.\times\left[\frac{\pi^2}{2} - \pi \tan^{-1}\left(\frac{r_e^2}{r_p^2}\left(\frac{P_p}{\eta_p P_s}\right)^{\frac{1}{2}}\right)\right]\right\}.
\end{aligned} \tag{14}$$

It could be possible to account for the further thinning of secondary transmitters due to the exclusion zones of other primary receivers. In that case, the density of secondary interferers seen by a primary receiver would be approximated to $\lambda_s p_r$ outside its exclusion zone. However, this is not considered to be consistent with the upper-bound approximations of section IV.

In order to calculate the corresponding expression for the secondary outage probability, we need to characterize the interference to SUs. $I_{p,s}$ is statistically identical to $I_{p,s}$ of scheme I, since the secondary exclusion zones do not alter the active PU distribution seen by SUs given the same primary exclusion zone radius. Thus, we use the Laplace transform $\mathcal{L}_{I_{p,s}}(s)$ calculated in (8). Finally, we approximate $I_{s,s}$ by recalling from [25] that, a type II MHP of density λ_s and *hard-core* distance r_g can be closely approximated to a PPP of density $\lambda_s p_g$. Therefore, assuming no secondary interferers within distance r_g and interferers distributed as a homogeneous PPP of reduced density $\lambda_s p_g$ beyond distance r_g gives a good approximation to $I_{s,s}$. Based on the discussion above, the left-hand side of the secondary outage constraint (3) can be approximated to,

$$\begin{aligned}
&\exp\left(-\frac{\eta_s N_0}{P_s r_s^{-\alpha}}\right) \mathcal{L}_{I_{s,s}}\left(\frac{\eta_s}{P_s r_s^{-\alpha}}\right) \mathcal{L}_{I_{p,s}}\left(\frac{\eta_s}{P_s r_s^{-\alpha}}\right) \\
&= \exp\left(\frac{-\eta_s N_0}{P_s r_s^{-\alpha}}\right) \exp\left(-2\pi\lambda_s p_g \int_{r_g}^{\infty} \frac{r}{1+\frac{r^\alpha r_s^{-\alpha}}{\eta_s}} dr\right) \\
&\quad \times \exp\left(-2\pi\lambda_p \int_{r_e-r_p-r_s}^{\infty} \frac{r}{1+\frac{r^\alpha P_s r_s^{-\alpha}}{\eta_s P_p}} dr\right).
\end{aligned} \tag{15}$$

Substituting $\alpha = 4$,

$$1-\epsilon_s \leq \exp\left(-\frac{\eta_s N_0}{P_s r_s^{-4}}\right)\exp\left\{-r_s^2\sqrt{\eta_s}\lambda_s \times \frac{1-\exp(-\lambda_s\pi r_g^2)}{\lambda_s\pi r_g^2}\left[\frac{\pi^2}{2}-\pi\tan^{-1}\left(\frac{r_g^2}{r_s^2\sqrt{\eta_s}}\right)\right]\right\} \times \exp\left\{-r_s^2\left(\frac{\eta_s P_p}{P_s}\right)^{\frac{1}{2}}\lambda_p \times\left[\frac{\pi^2}{2}-\pi\tan^{-1}\left(\left(\frac{r_e-r_p-r_s}{r_s}\right)^2\left(\frac{P_s}{\eta_s P_p}\right)^{\frac{1}{2}}\right)\right]\right\}. \quad (16)$$

Proposition 1: Given the same primary exclusion zone radius and same active secondary transmitter density, the secondary outage probability in scheme II is lower than that in scheme I.

Proof: To ensure the same active secondary transmitter density, $p_t = [1-\exp(-\lambda_s\pi r_g^2)]/(\lambda_s\pi r_g^2)$. Let us denote the secondary success probability in scheme I (given on the right-hand-side of (9)) as $1-\epsilon_s^{(I)}$, and denote the secondary success probability in scheme II (given on the right-hand-side of (16)) as $1-\epsilon_s^{(II)}$. Then we have the following ratio:

$$\frac{1-\epsilon_s^{(II)}}{1-\epsilon_s^{(I)}} = \exp\left[\pi\lambda_s p_t\sqrt{\eta_s}r_s^2\tan^{-1}\left(\frac{r_g^2}{r_s^2\sqrt{\eta_s}}\right)\right] \geq 1 \quad (17)$$

which proves $\epsilon_s^{(I)} \geq \epsilon_s^{(II)}$. ■

Expressions (14) and (16) relate the outage probabilities to the radii of the exclusion zones. We can express them in the form of $P_2(r_g, r_e) \geq 0$ and $S_2(r_g, r_e) \geq 0$ respectively. Based on these inequalities, the solution to the following problem gives the maximum retaining probability satisfying the outage constraints for $\alpha = 4$ case.

Problem 2:

$$\max_{\substack{r_g^{max}\geq r_g\geq 0\\ r_e^{max}\geq r_e\geq r_p+r_s}} p_r(r_g,r_e) = \frac{1-\exp(-\lambda_s\pi r_g^2)}{\lambda_s\pi r_g^2}\exp(-\lambda_p\pi r_e^2)$$

subject to,

$$P_2(r_g, r_e) \geq 0$$
$$S_2(r_g, r_e) \geq 0.$$

We propose a solution to Problem 2, by making the following observations. First, to ensure that Problem 2 is feasible for all r_e, let us assume $P_2(r_g^{max}, r_e), S_2(r_g^{max}, r_e) \geq 0$, $\forall r_e \in [r_p + r_s, r_e^{max}]$. This means, sufficiently large secondary exclusion zones alone should satisfy the outage constraints.

Lemma 4: For a given $r_e \in [r_p + r_s, r_e^{max}]$, there exists a greatest lower bound $N(r_e) \leq r_g^{max}$ on r_g, such that $r_g \in [N(r_e), r_g^{max}]$ satisfies $P_2(r_g, r_e) \geq 0$ and $S_2(r_g, r_e) \geq 0$, while $r_g < N(r_e)$ violates at least one of these constraints or the implicit constraint $r_g \in [0, r_g^{max}]$.

Proof: Although a closed form expression for $N(r_e)$ does not exist, we can prove the existence of $N(r_e)$ by i) using the assumption that $r_g = r_g^{max}$ always satisfies the constraints, and ii) showing that $P_2(r_g, r_e)$ and $S_2(r_g, r_e)$ are monotone increasing functions of r_g over $r_g \in [0, r_g^{max}]$. $P_2(r_g, r_e)$ increases with r_g if $p_g = [1-\exp(-\lambda_s\pi r_g^2)]/(\lambda_s\pi r_g^2)$ is a decreasing function of r_g (see (14)). We make the change of variable $v = \lambda_s\pi r_g^2$ for simplicity, and look for the first order derivative of p_g with respect to $v > 0$;

$$\frac{dp_g(v)}{dv} = \frac{ve^{-v}+e^{-v}-1}{v^2}. \quad (18)$$

After some algebraic manipulations, we arrive at the following bi-conditional statement,

$$\frac{dp_g(v)}{dv} \leq 0 \Leftrightarrow e^v \geq 1+v \quad \forall v \geq 0. \quad (19)$$

The latter condition is satisfied for all $v \geq 0$, and therefore p_g is a monotone decreasing function of r_g and hence $P_2(r_g, r_e)$ is a monotone increasing function of r_g over its domain. Similarly, $S_2(r_g, r_e)$ increases with r_g, since both p_g and $\left[\frac{\pi^2}{2}-\pi\tan^{-1}\left(\frac{r_g^2}{r_s^2\sqrt{\eta_s}}\right)\right]$ are decreasing functions of r_g over $r_g \in [0, r_g^{max}]$ (see (16)). ■

Lemma 5: The maximum retaining probability p_r, lies on the boundary of the feasible region described by the points $(N(r_e), r_e)$, $\forall r_e \in [r_p + r_s, r_e^{max}]$.

Proof: Let us assume the contrary where the optimal point (r_g', r_e') is strictly inside the feasible region such that $r_g' > N(r_e')$. Then, there exist some smaller $r_g'' \in [N(r_e'), r_g')$ such that (r_g'', r_e') is feasible. Also note that the objective $p_r(r_g, r_e) = p_g p_e$ is a monotone decreasing function of r_g, as p_g decreases with increasing r_g as shown in the proof of Lemma 4. Then, $p_r(r_g'', r_e') > p_r(r_g', r_e')$ and (p_t', r_e') cannot be optimal. ■

Therefore, the optimal point in Problem 2 can be found numerically by calculating $N(r_e)$, e.g. by bisection method, and then selecting the point among $(N(r_e), r_e)$ over $r_e \in [r_p + r_s, r_e^{max}]$ leading to the largest objective value. Figure 4 shows the feasible region and the optimal point for given parameters.

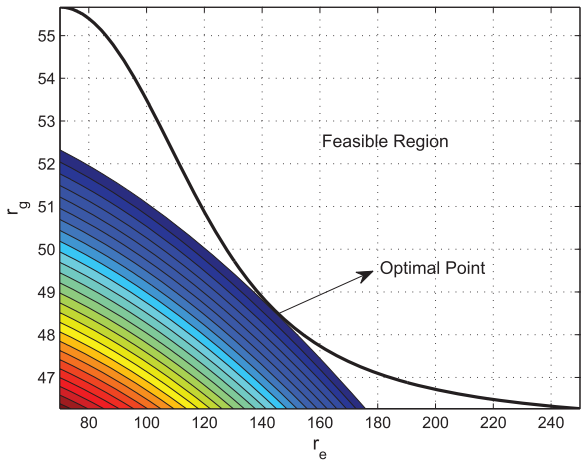

Fig. 4. The contour plot of the transmission capacity (decreases from red to blue) and the boundary of the feasible region $r_g = N(r_e)$. $P_p = 3$ W, $P_s = 0.1$ W, $\lambda_p = 3\times10^{-6}$, $\lambda_s = 10^{-3}$, $N = 10^{-12}$ W, $\alpha = 4$, $r_p = 50$ m, $r_s = 20$ m, $\epsilon_p = 0.1$, $\epsilon_s = 0.1$, $\eta_p = \eta_s = 3$.

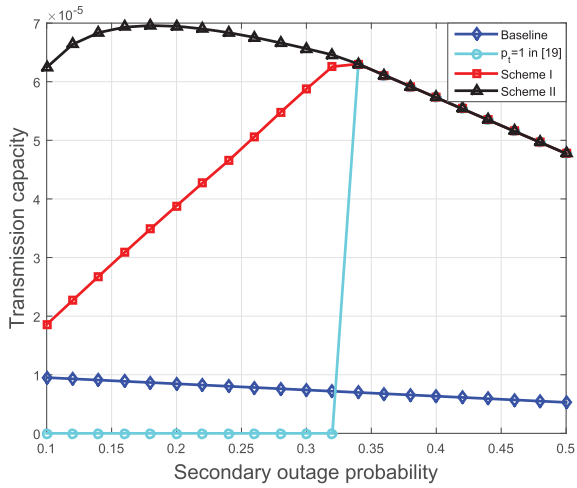

Fig. 5. Optimized transmission capacity of the secondary network versus the secondary outage probability, with $P_p = 3\ W$, $P_s = 0.1\ W$, $\lambda_p = 3 \times 10^{-6}$, $\lambda_s = 10^{-4}$, $N = 10^{-12}\ W$, $\alpha = 4$, $r_p = 50\ m$, $r_s = 20\ m$, $\epsilon_p = 0.1$, $\eta_p = \eta_s = 3$.

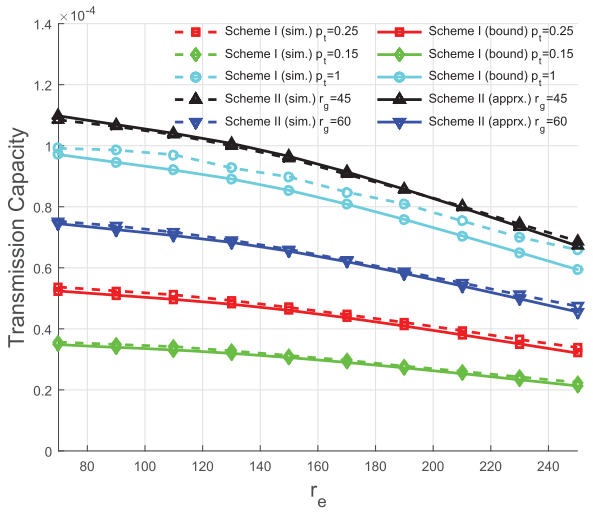

Fig. 6. Effects of r_e, r_g (in meters) and p_t on the secondary network transmission capacity, with no outage constraints. $P_p = 3\ W$, $P_s = 0.1\ W$, $\lambda_p = 3 \times 10^{-6}$, $\lambda_s = 3 \times 10^{-4}$, $N = 10^{-12}\ W$, $\alpha = 4$, $r_p = 50\ m$, $r_s = 20\ m$, $\eta_p = \eta_s = 3$.

VI. Simulations

This section compares the performance of the proposed schemes and validates the analytical results through numerical simulations. First, the transmission capacity (in terms of the successful transmissions per resource block per m^2) of the three schemes is compared in Figure 5 for varying secondary outage probability values. All data points shown in this figure are drawn from the analytical results with optimized p_t in baseline, optimized r_e when $p_t = 1$ as in [19], jointly optimized (p_t, r_e) in scheme I and jointly optimized (r_g, r_e) in scheme II to maximize the retaining probability under outage constraints. In the baseline scheme, the transmission capacity decays with increasing ϵ_s because the density of active SUs in simple underlay is typically limited by the primary outage constraint. Relaxing the secondary outage constraint therefore, does not increase the active SU density. Similarly, below a certain ϵ_s, the density of active SUs in [19] is limited by the secondary outage constraint and no feasible solution exists to design r_e alone when $p_t = 1$. On the other hand, joint optimization of p_t and r_e in scheme I ensures a feasible solution, even when the secondary outage constraint is tight. Increasing ϵ_s beyond 0.34 in scheme I and scheme in [19] sufficiently relaxes the secondary outage constraint and the active SU density becomes limited by the primary outage constraint. This transition of the limiting constraint from secondary to primary outage constraint is the reason for the jump in scheme in [19], and the kink in scheme I at $\epsilon_s = 0.34$.

The significant performance gap between scheme I and II suggests that, having primary exclusion zones alone does not improve the capacity much, when the secondary network capacity is dominated by the interference received from other SUs. Employing additional secondary exclusion between SUs gives the highest transmission capacity when the density of active SU is limited by the secondary outage constraint. At sufficiently large ϵ_s the three schemes perform the same since the primary outage constraint is the limiting factor.

The following figures investigate the accuracy of the analytical results on schemes I and II, by simulating the channel access protocols numerically. For each data point in numerical simulations, MatLab is used to generate 50, 000 independent network realizations. The deployment area is selected large enough, such that further increasing the area does not cause any noticeable difference on the results. Three metrics are calculated by averaging over the network realizations: i) secondary network capacity, ii) secondary outage probability, iii) primary outage probability. The SUs are active/inactive based on their channel access protocol. The outage probabilities are calculated as the ratio of users with SINR ratios below the threshold. As consistent with the system model, the transmission capacity of the secondary network is calculated by dividing the number of successful (SINR ratios above the threshold) secondary transmissions to the deployment area.

Figure 6 and 7 analyze the secondary network transmission capacity and outage probability respectively for several optimization variable ((p_t, r_e) and (r_g, r_e)) pairs. For both schemes, as r_e increases the outage probability decreases (Fig. 7). This is because less SUs are activated and also the SUs get further apart from PUs as r_e increases. However, the decrease in the secondary transmitter density dominates the decrease in secondary outage probability and the capacity decreases (Fig. 6) with increasing r_e. In general, adopting secondary exclusion zones in addition to the primary exclusion zones results in higher capacity and lower outage probability values than having the primary exclusion zones alone.

Regarding scheme I, the analytical results are the lower bounds for the capacity and upper bounds for the secondary outage probability as discussed in section IV. The limited difference between the analytical bounds and numerical simulations is caused mainly due to the modeling of secondary transmitters $r_e - r_p - r_s$ away from the primary receivers as a homogeneous PPP. Choosing $p_t = 1$ results in more active SUs, but much larger outage probability as compared to choosing

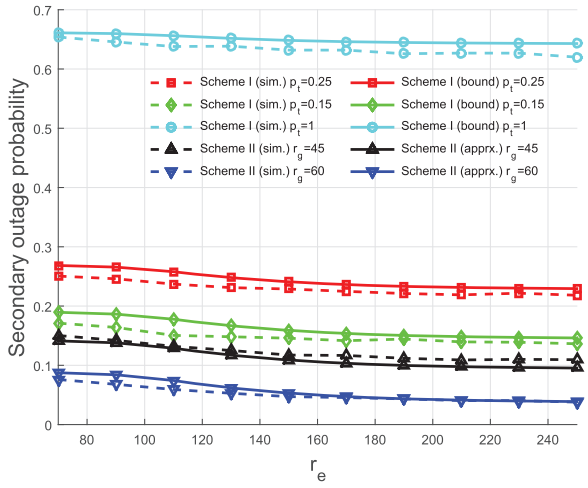

Fig. 7. Effects of r_e, r_g (in meters) and p_t on the secondary outage probability. $P_p = 3\ W$, $P_s = 0.1\ W$, $\lambda_p = 3 \times 10^{-6}$, $\lambda_s = 3 \times 10^{-4}$, $N = 10^{-12}\ W$, $\alpha = 4$, $r_p = 50$ m, $r_s = 20$ m, $\eta_p = \eta_s = 3$.

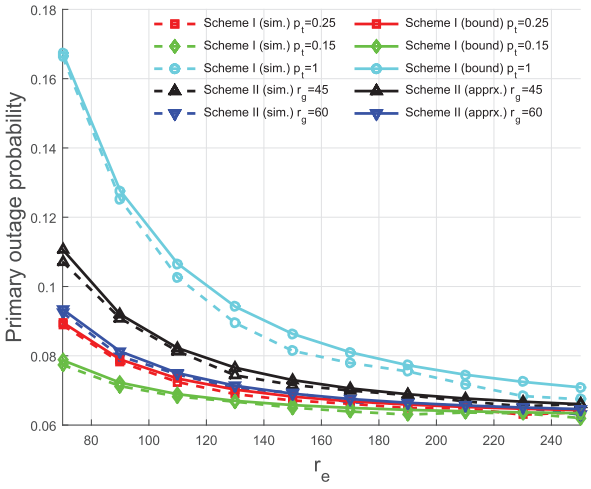

Fig. 8. Effects of r_e, r_g (in meters) and p_t on the primary outage probability. $P_p = 3\ W$, $P_s = 0.1\ W$, $\lambda_p = 3 \times 10^{-6}$, $\lambda_s = 3 \times 10^{-4}$, $N = 10^{-12}\ W$, $\alpha = 4$, $r_p = 50$ m, $r_s = 20$ m, $\eta_p = \eta_s = 3$.

$p_t = 0.25$ and especially $p_t = 0.15$ since the interference is larger as p_t increases. The decrease in the active secondary transmitter density when moving from $p_t = 1$ to $p_t = 0.15$ dominates the decrease in the outage probability, and hence the capacity is smaller for lower p_t values. However, note that the $p_t = 1$ case is not feasible because it leads to very large secondary outage probability.

In scheme II, the analytical results are the approximations on the capacity and secondary outage probability. The main cause of the error is the approximation that the retained transmitters farther than r_g to each secondary receiver are modeled as a homogeneous PPP. With $r_g = 45$, the capacity is greater than that of $r_g = 60$ because the active secondary transmitter are denser for smaller r_g, and the decrease in the secondary outage probability from $r_g = 45$ to $r_g = 60$ cannot compensate for the decrease in the active node density.

Figure 8 shows the impact of the optimization variables on the primary outage probability. In scheme I plots, the analytical

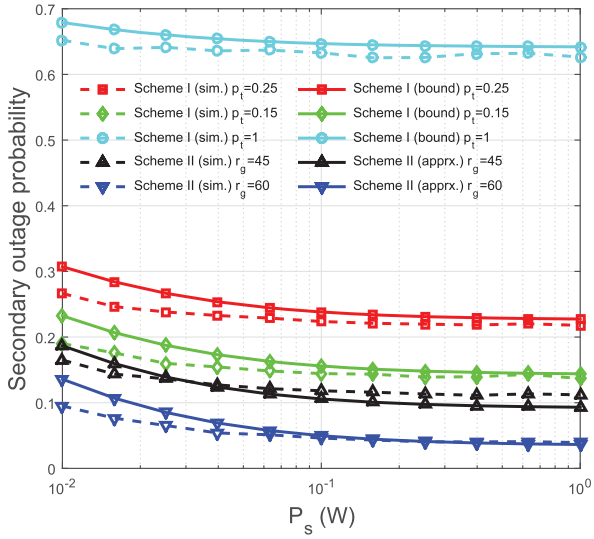

Fig. 9. Effect of P_s (in Watts) on the secondary outage probability. $r_e = 160$ m $P_p = 3\ W$, $\lambda_p = 3 \times 10^{-6}$, $\lambda_s = 3 \times 10^{-4}$, $N = 10^{-12}\ W$, $\alpha = 4$, $r_p = 50$ m, $r_s = 20$ m, $\eta_p = \eta_s = 3$.

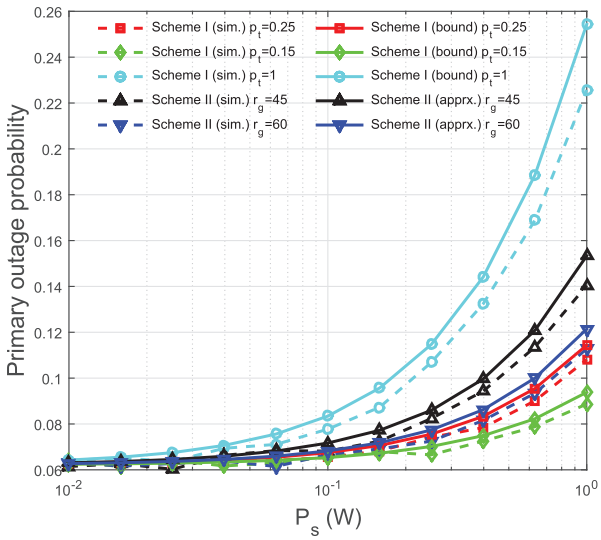

Fig. 10. Effect of P_s (in Watts) on the primary outage probability. $r_e = 160\ m$ $P_p = 3\ W$, $\lambda_p = 3 \times 10^{-6}$, $\lambda_s = 3 \times 10^{-4}$, $N = 10^{-12}\ W$, $\alpha = 4$, $r_p = 50$ m, $r_s = 20$ m, $\eta_p = \eta_s = 3$.

data points are upper bounds on the actual simulation results, while in scheme II analytical results are simply approximations. The errors are caused due to the modeling of secondary transmitters farther than r_e to a typical primary receiver as a homogeneous PPP.

The primary outage probability is lower for $p_t = 0.15$ and $r_g = 60$ cases since the effective active SU density is less as compared to $p_t = 0.25$ and $r_g = 45$ cases respectively. For $p_t = 1$ case primary outage probability is the largest due to all secondary transmitters outside the primary exclusion zone being active. As r_e increases, primary receivers are further separated from the active secondary transmitters and also the active secondary transmitter density decreases. Consequently, the interference from the secondary network and hence the primary outage probability decreases. At large r_e values, the

outage probability is around $\epsilon_p = 0.065$ for all cases, because the interference is caused mainly by the primary transmitters. The primary outage probability can be further reduced only if an interference management technique (e.g., exclusion zones) within the primary network is used.

Finally, Figures 9 and 10 investigate the effects of SU transmit power P_s on the secondary and primary outage probabilities respectively. As P_s increases, the signal strength and interference from SUs increase proportionally while the interference from primary transmitters and the noise power remains the same. As a result, ϵ_s degrades as P_s increases. The transmission capacity increases proportional to the increase in $1 - \epsilon_s$ due to the fact that average density of active secondary transmitters is unchanged. In Figure 10, the primary outage probability increases due to proportional increase in the interference caused by the secondary network as P_s increases.

VII. Conclusion

In a wireless environment with two co-existing systems, we proposed the use of CR concepts for interference management through spatial spectrum sharing. Depending on the availability of different cognitive information in the secondary-tier, we proposed three spectrum sharing schemes. In the simple underlay, SUs transmit independently regardless of the activity of nearby users. Then, the primary exclusion zones were introduced to protect the primary receivers from neighboring secondary transmitters. Finally, a CSMA-type protocol for the secondary network was incorporated into the primary exclusion zones. The locations of the active secondary transmitters in this novel scheme form a MHP with holes centered at primary receivers. The analytical expressions to closely approximate the optimal primary and secondary exclusion zone radii and transmission probability were presented. The simulations have shown that, the primary exclusion zones significantly reduce the interference across the primary and secondary networks, while the secondary exclusion zones are critical in mitigating the interference within the secondary network.

Appendix A
Proof of Lemma 1

The left-hand side of (1) can be evaluated as,

$$\begin{aligned}
&\Pr\left[h_p \geq \frac{\eta_p}{P_p r_p^{-\alpha}}(N_0 + I_{s,p} + I_{p,p})\right] \\
&= \exp\left(-\frac{\eta_p N_0}{P_p r_p^{-\alpha}}\right)\mathbb{E}\left[\exp\left(-\frac{\eta_p I_{s,p}}{P_p r_p^{-\alpha}}\right)\exp\left(-\frac{\eta_p I_{p,p}}{P_p r_p^{-\alpha}}\right)\right] \\
&= \exp\left(-\frac{\eta_p N_0}{P_p r_p^{-\alpha}}\right) \\
&\quad \times \mathbb{E}\left[\exp\left(-\frac{\eta_p I_{s,p}}{P_p r_p^{-\alpha}}\right)\right]\mathbb{E}\left[\exp\left(-\frac{\eta_p I_{p,p}}{P_p r_p^{-\alpha}}\right)\right] \qquad (20)
\end{aligned}$$

where the first equality follows from the complementary cumulative distribution function (CCDF) of the exponential random variable h_p and the second equality from the independence of $I_{s,p}$ and $I_{p,p}$. By definition, $\mathbb{E}[\exp(-\eta_p I_{s,p}/P_p r_p^{-\alpha})]$ and $\mathbb{E}[\exp(-\eta_p I_{p,p}/P_p r_p^{-\alpha})]$ are the Laplace transforms of the PDFs of $I_{s,p}$ and $I_{p,p}$ evaluated at $s = \eta_p/P_p r_p^{-\alpha}$. These transforms were already calculated for homogeneous PPP distributed interferers in the case of Rayleigh fading. Using Eqn. (8) in [26], the rightmost-hand side of (20) can be evaluated as,

$$\begin{aligned}
&\exp\left(-\frac{\eta_p N_0}{P_p r_p^{-\alpha}}\right)\mathcal{L}_{I_{s,p}}\left(\frac{\eta_p}{P_p r_p^{-\alpha}}\right)\mathcal{L}_{I_{p,p}}\left(\frac{\eta_p}{P_p r_p^{-\alpha}}\right) \\
&= \exp\left(-\eta_p N_0/P_p r_p^{-\alpha}\right)\exp\left(-\lambda_{s,e} P_s^{\delta}\eta_p^{\delta} r_p^2 K_\alpha / P_p^{\delta}\right) \\
&\quad \times \exp(-\lambda_p \eta_p^{\delta} r_p^2 K_\alpha). \qquad (21)
\end{aligned}$$

Here, $\lambda_{s,e} = \lambda_s p_t$ represents the effective density of active secondary transmitters satisfying the primary outage constraint. Substituting (21) into (1), we find that

$$\lambda_{s,e} \leq -\frac{P_p^{\delta}}{P_s^{\delta}\eta_p^{\delta} r_p^2 K_\alpha}\left[\ln(1-\epsilon_p) + \frac{\eta_p N_0}{P_p r_p^{-\alpha}}\right] - \lambda_p \frac{P_p^{\delta}}{P_s^{\delta}} \qquad (22)$$

and $p_t = \lambda_{s,e}/\lambda_s$.

Appendix B
Proof of Lemma 2

As in the proof of Lemma 1, the left-hand side of (3) can be expressed in terms of the Laplace transforms of the PDFs of interference terms,

$$\begin{aligned}
&\Pr\left[h_s \geq \frac{\eta_s}{P_s r_s^{-\alpha}}(N_0 + I_{s,s} + I_{p,s})\right] \\
&= \exp\left(-\frac{\eta_s N_0}{P_s r_s^{-\alpha}}\right)\mathcal{L}_{I_{s,s}}\left(\frac{\eta_s}{P_s r_s^{-\alpha}}\right)\mathcal{L}_{I_{p,s}}\left(\frac{\eta_s}{P_s r_s^{-\alpha}}\right) \\
&= \exp\left(-\eta_s N_0/P_s r_s^{-\alpha}\right)\exp\left(-\lambda_{s,e}\eta_s^{\delta} r_s^2 K_\alpha\right) \\
&\quad \times \exp\left(-\lambda_p P_p^{\delta}\eta_s^{\delta} r_s^2 K_\alpha / P_s^{\delta}\right). \qquad (23)
\end{aligned}$$

Thus, we have

$$\lambda_{s,e} \leq -\frac{\ln(1-\epsilon_s) + \frac{\eta_s N_0}{P_s r_s^{-\alpha}}}{\eta_s^{\delta} r_s^2 K_\alpha} - \lambda_p \frac{P_p^{\delta}}{P_s^{\delta}}, \qquad (24)$$

with $p_t = \lambda_{s,e}/\lambda_s$.

References

[1] A. Goldsmith, S. Jafar, I. Maric, and S. Srinivasa, "Breaking spectrum gridlock with cognitive radios: An information theoretic perspective," *Proc. IEEE*, vol. 97, no. 5, pp. 894–914, May 2009.

[2] S. P. Weber, X. Yang, J. Andrews, and G. de Veciana, "Transmission capacity of wireless ad hoc networks with outage constraints," *IEEE Trans. Inf. Theory*, vol. 51, no. 12, pp. 4091–4102, Dec. 2005.

[3] A. Hasan and J. Andrews, "Scheduling using near-optimal guard zones for CDMA ad hoc networks," in *Proc. IEEE Int. Conf. Commun.*, Jun. 2006, vol. 9, pp. 4002–4007.

[4] A. Hulbert, "Spectrum sharing through beacons," in *Proc. 16th Int. Symp. Pers. Indoor Mobile Radio Commun.*, Sep. 2005, vol. 2, pp. 989–993.

[5] M. Fitch, M. Nekovee, S. Kawade, K. Briggs, and R. MacKenzie, "Wireless service provision in TV white space with cognitive radio technology: A telecom operator's perspective and experience," *IEEE Commun. Mag.*, vol. 49, no. 3, pp. 64–73, Mar. 2011.
[6] G. Alfano, M. Garetto, and E. Leonardi, "New directions into the stochastic geometry analysis of dense CSMA networks," *IEEE Trans. Mobile Comput.*, vol. 13, no. 2, pp. 324–336, Feb. 2014.
[7] A. Hasan and J. Andrews, "The guard zone in wireless ad hoc networks," *IEEE Trans. Wireless Commun.*, vol. 6, no. 3, pp. 897–906, Mar. 2007.
[8] J. Chen, M. Ding, and Q. Zhang, "Interference statistics and performance analysis of MIMO ad hoc networks in binomial fields," *IEEE Trans. Veh. Technol.*, vol. 61, no. 5, pp. 2033–2043, Jun. 2012.
[9] D. Torrieri and M. Valenti, "Exclusion and guard zones in DS-CDMA ad hoc networks," *IEEE Trans. Commun.*, vol. 61, no. 6, pp. 2468–2476, Jun. 2013.
[10] J. G. Andrews, F. Baccelli, and R. K. Ganti, "A tractable approach to coverage and rate in cellular networks," *IEEE Trans. Commun.*, vol. 59, no. 11, pp. 3122–3134, Nov. 2011.
[11] S.-M. Cheng, W. C. Ao, F.-M. Tseng, and K.-C. Chen, "Design and analysis of downlink spectrum sharing in two-tier cognitive FEMTO networks," *IEEE Trans. Veh. Technol.*, vol. 61, no. 5, pp. 2194–2207, Jun. 2012.
[12] S.-R. Cho and W. Choi, "Energy-efficient repulsive cell activation for heterogeneous cellular networks," *IEEE J. Sel. Areas Commun.*, vol. 31, no. 5, pp. 870–882, May 2013.
[13] C. Jia and T. J. Lim, "Designing femtocell exclusion zones to minimize power in a heterogeneous network," in *Proc. IEEE Global Commun. Conf.*, Dec. 2014, pp. 4251–4256.
[14] D. Cabric, S. Mishra, and R. Brodersen, "Implementation issues in spectrum sensing for cognitive radios," in *Proc. Conf. Rec. 38th Asilomar Conf. Signals Syst. Comput.*, Nov. 2004, vol. 1, pp. 772–776.
[15] X. Hong, C.-X. Wang, and J. Thompson, "Interference modeling of cognitive radio networks," in *Proc. IEEE Veh. Technol. Conf.*, May 2008, pp. 1851–1855.
[16] M. Vu, N. Devroye, and V. Tarokh, "On the primary exclusive region of cognitive networks," *IEEE Trans. Wireless Commun.*, vol. 8, no. 7, pp. 3380–3385, Jul. 2009.
[17] A. Ghasemi and E. Sousa, "Interference aggregation in spectrum-sensing cognitive wireless networks," *IEEE J. Sel. Topics Signal Process.*, vol. 2, no. 1, pp. 41–56, Feb. 2008.
[18] A. Kahlon, S. Periyalwar, H. Yanikomeroglu, and S. Szyszkowicz, "Outage in a cellular network overlaid with an ad hoc network: The uplink case," in *Proc. IEEE 22nd Symp. Int. Pers. Indoor Mobile Radio Commun.*, Sep. 2011, pp. 588–592.
[19] C. H. Lee and M. Haenggi, "Interference and outage in poisson cognitive networks," *IEEE Trans. Wireless Commun.*, vol. 11, no. 4, pp. 1392–1401, Apr. 2012.
[20] M. Haenggi and R. K. Ganti, "Interference in large wireless networks," in *Foundations and Trends in Networking*, NOW Publishers, vol. 3, no. 2, pp. 127–248, 2008.
[21] S. Weber, J. Andrews, and N. Jindal, "An overview of the transmission capacity of wireless networks," *IEEE Trans. Commun.*, vol. 58, no. 12, pp. 3593–3604, Dec. 2010.
[22] D. Stoyan, W. S. Kendall, J. Mecke, and L. Ruschendorf, *Stochastic Geometry and Its Applications*. Hoboken, NJ, USA: Wiley, 1987, vol. 2.
[23] L. Wang and V. Fodor, "On the gain of primary exclusion region and vertical cooperation in spectrum sharing wireless networks," *IEEE Trans. Veh. Technol.*, vol. 61, no. 8, pp. 3746–3758, Oct. 2012.
[24] B. Matérn, *Spatial Variation*, 2nd ed. New York, NY, USA: Springer, 1986.
[25] M. Haenggi, "Mean interference in hard-core wireless networks," *IEEE Commun. Lett.*, vol. 15, no. 8, pp. 792–794, Aug. 2011.
[26] M. Haenggi, J. Andrews, F. Baccelli, O. Dousse, and M. Franceschetti, "Stochastic geometry and random graphs for the analysis and design of wireless networks," *IEEE J. Sel. Areas Commun.*, vol. 27, no. 7, pp. 1029–1046, Sep. 2009.

Utku Tefek (S'13) received the B.Sc. degree (with high Hons.) in electrical and electronics engineering from Bilkent University, Ankara, Turkey, in 2013. He is currently pursuing the Ph.D. degree in electrical and computer engineering at the National University of Singapore, Singapore. His research interests include cognitive radio, machine-to-machine communications, and the application of stochastic models to wireless networks.

Teng Joon Lim (S'92–M'95–SM'12) received the B.Eng. degree (with first class Hons.) in electrical engineering from the National University of Singapore, Singapore, and the Ph.D. degree from the University of Cambridge, Cambridge, U.K., in 1992 and 1996, respectively. From September 1995 to November 2000, he was a Researcher with the Centre for Wireless Communications, Singapore, one of the predecessors of the Institute for Infocomm Research (I2R). From December 2000 to May 2011, he was an Assistant Professor, an Associate Professor, and then a Professor with the Edward S. Rogers Sr. Department of Electrical and Computer Engineering, University of Toronto, Toronto, ON, Canada. Since June 2011, he has been a Professor with the Department of Electrical and Computer Engineering, National University of Singapore, where he served as the Deputy Head (Research and Graduate Programs) from July 2014 to August 2015. He currently serves as the Vice-Dean (Graduate Programmes) in the Faculty of Engineering. His research interests include Internet of Things, heterogeneous networks, cooperative transmission, energy-optimized communication networks, multicarrier modulation, MIMO, cooperative diversity, cognitive radio, and stochastic geometry for wireless networks. He is an Area Editor (in the Wireless Communications Theory and Systems I area) of the IEEE TRANSACTIONS ON WIRELESS COMMUNICATIONS, and previously served as an Associate Editor for the same journal. He is serving as an Associate Editor for the IEEE WIRELESS COMMUNICATIONS LETTERS, and an Executive Editor for *Transactions on Emerging Telecommunications Technologies* (ETT) (Wiley). Previously, he was an Associate Editor for the IEEE SIGNAL PROCESSING LETTERS and for the IEEE TRANSACTIONS ON VEHICULAR TECHNOLOGY. He has also co-chaired a number of IEEE conferences, and is a regular TPC member at major international conferences.